

The magnetic resonance in high-temperature superconductors: evidence for an extended s-wave pairing symmetry

GUO-MENG ZHAO†

Department of Physics and Astronomy, California State University at
Los Angeles, Los Angeles, CA 90032, USA

[Received 17 May 2004 and accepted 28 May 2004]

ABSTRACT

We have identified several important features in the neutron scattering data of cuprates that are difficult to explain in terms of d-wave and isotropic s-wave order parameters. Alternatively, we show that the neutron data are in quantitative agreement with an order parameter that has an extended s-wave (A_{1g}) symmetry and opposite sign in the bonding and antibonding electron bands formed within the Cu_2O_4 bilayers. The extended s wave has eight line nodes and changes sign when a node is crossed. This A_{1g} pairing symmetry may be compatible with a charge-fluctuation-mediated pairing mechanism.

The microscopic pairing mechanism responsible for high-temperature superconductivity in copper-based perovskite oxides is still a subject of intense debate despite tremendous experimental and theoretical efforts for over 15 years. The debate has been centred around the role of antiferromagnetic spin fluctuations in high-temperature superconductivity and the gap symmetry. The gap symmetry of the superconducting, which is often called the order parameter symmetry, reflects the underlying pairing mechanism. Extensive inelastic neutron scattering experiments have accumulated a great deal of important data that should be sufficient to address these central issues. Of particular interest is the magnetic resonance peak that has been observed in double-layer cuprate superconductors such as $YBa_2Cu_3O_y$ (YBCO) (Bourges *et al.* 1995, 1996, 1999, Bourges 1998, Fong *et al.* 1995, Dai *et al.* 2001) and $Bi_2Sr_2CaCu_2O_{8+y}$ (BSCCO) (Fong *et al.* 1999, He *et al.* 2001), and in a single-layer compound $Tl_2Ba_2CuO_{6+y}$ (Tl-2201) (He *et al.* 2002). A number of theoretical models (Demler and Zhang 1995, Morr and Pines 1998, Abanov and Chubukov 1999, Brinckmann and Lee 1999) have been proposed to explain the magnetic resonance peak in terms of d-wave magnetic pairing mechanisms. These theories can qualitatively explain some features of the neutron data, but it is particularly difficult to account for an important feature: the magnetic resonance in optimally and overdoped double-layer cuprates is much more pronounced in the odd channel than in the even channel (Fong *et al.* 1995, Bourges *et al.* 1996, Bourges 1998). In order to overcome this difficulty, Mazin and Yakovenko (1995) proposed an order parameter that has isotropic s-wave symmetry and opposite sign in the bonding

†Email: gzhao@calstatela.edu.

and antibonding electron bands formed within the Cu_2O_4 bilayers. However, this model predicts that the resonance energy is larger than twice the magnitude of the superconducting gap along the Cu–O bonding direction, in disagreement with experiment. Further, the nodeless *s*-wave gap symmetry is inconsistent with the measurements of the penetration depth, thermal conductivity and specific heat, which consistently suggest the existence of line nodes in the gap function of hole-doped cuprates (Hardy *et al.* 1993, Chiao *et al.* 2000).

Here we identify several important features in the neutron scattering data of cuprates. These features are inconsistent with the *d*-wave order parameter (OP). Alternatively, we show that the neutron data are in quantitative agreement with an order parameter that has an extended *s*-wave (A_{1g}) symmetry (Zhao 2001, Brandow 2002) and opposite sign in the bonding and antibonding electron bands formed within the Cu_2O_4 bilayers (Mazin and Yakovenko 1995).

The magnetic resonance peak observed in optimally doped and overdoped double-layer compounds $\text{YBa}_2\text{Cu}_3\text{O}_y$ (Bourges *et al.* 1995, 1996, 1999, Fong *et al.* 1995, Bourges 1998) and $\text{Bi}_2\text{Sr}_2\text{CaCu}_2\text{O}_{8+y}$ (Fong *et al.* 1999, He *et al.* 2001) is a sharp collective mode that occurs at an energy of 38–43 meV and at the two-dimensional wavevector $\mathbf{Q}_{\text{AF}} = (\pi/a, \pi/a)$, where a is the nearest-neighbour Cu–Cu distance. Figure 1(a) shows the imaginary part of the odd channel spin susceptibility as a function of excitation energy for a slightly underdoped double-layer compound $\text{YBa}_2\text{Cu}_3\text{O}_{6.92}$. The figure is reproduced from Bourges *et al.* (1999). There are several striking features in the data. (a) The resonance peak at $E_r = 41$ meV appears below T_c and this resonance peak intensity in the superconducting state $I_{\text{odd}}^{\text{S}}(E_r)$ is larger than the normal-state intensity $I_{\text{odd}}^{\text{N}}(E_r)$ by a factor of about 3.6, i.e. $I_{\text{odd}}^{\text{S}}(E_r)/I_{\text{odd}}^{\text{N}}(E_r) = 3.6$. (b) A spin gap feature is seen below T_c and there is a small shoulder that occurs at an energy slightly above the spin gap energy $E_g = 32$ meV. Figure 1(b) shows a q_l scan at $E = 40$ meV in $\text{YBa}_2\text{Cu}_3\text{O}_{6.92}$ displaying a modulation typical of odd excitation. The figure is reproduced from Bourges (1998). From figure 1(b), we find feature (c): the odd-channel magnetic resonance intensity within the Cu_2O_4 bilayers is larger than the even-channel intensity by a factor of about 5 (Bourges 1998), i.e. $I_{\text{odd}}^{\text{S}}(E_r)/I_{\text{even}}^{\text{S}}(E_r) = 5$. From neutron studies on different double-layer compounds with different doping levels, one identifies feature (d): the resonance energy E_r does not increase with doping in the overdoped range, but is proportional to T_c as $E_r/k_B T_c \simeq 5.2$ in both underdoped and overdoped ranges (He *et al.* 2001).

On the other hand, the neutron data for single-layer Tl-2201 are different from those for double-layer compounds. For single-layer Tl-2201, we show in figure 2(a) the difference spectrum of the neutron intensities at $T = 27$ K ($< T_c$) and $T = 99$ K ($> T_c$), at a wavevector of $\mathbf{Q} = (0.5, 0.5, 12.25)$. The figure is reproduced from He *et al.* (2002). Although a sharp peak feature is clearly seen at $E_r = 46$ meV, it is remarkable that the peak intensity in the superconducting state is close to the magnetic neutron intensity in the normal state, that is, $I^{\text{S}}(E_r)/I^{\text{N}}(E_r) \simeq 1$. This is in sharp contrast with the above result for the double-layer compound $\text{YBa}_2\text{Cu}_3\text{O}_{6.92}$, where we found $I_{\text{odd}}^{\text{S}}(E_r)/I_{\text{odd}}^{\text{N}}(E_r) = 3.6$. Thus we identify feature (e) as $I^{\text{S}}(E_r)/I^{\text{N}}(E_r) \simeq 1$ for the single-layer compound.

We should mention that feature (e) identified for single-layer Tl-2201 is valid only if the non-magnetic background has a negligible temperature dependence below 100 K. It is known that nuclear contributions predominantly constitute the main part of the neutron signal (Bourges *et al.* 1996). Any nuclear contributions (non-magnetic

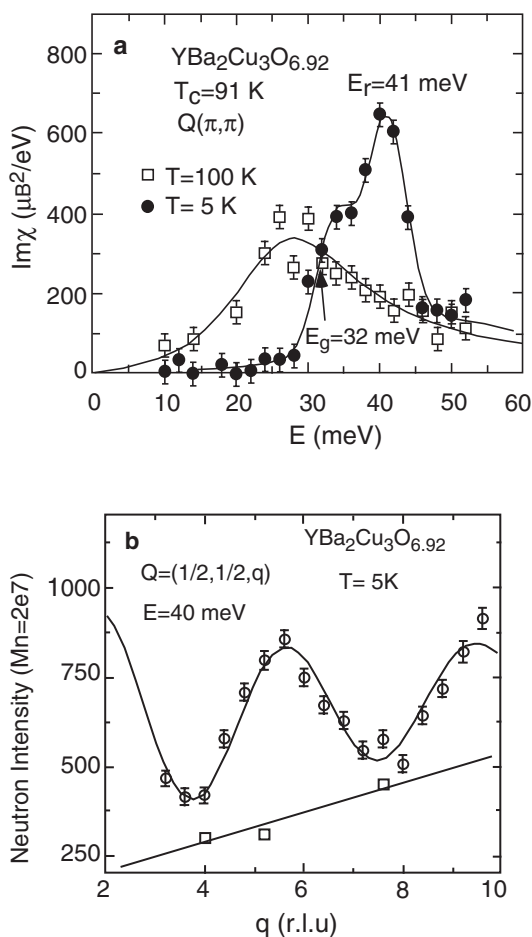


Figure 1. (a) The imaginary part of the dynamic spin susceptibility as a function of excitation energy for $\text{YBa}_2\text{Cu}_3\text{O}_{6.92}$ in the normal and superconducting states (reproduced from Bourges *et al.* (1999)). (b) q_l scan at $E = 40\text{ meV}$ in $\text{YBa}_2\text{Cu}_3\text{O}_{6.92}$ displaying a modulation typical of odd excitation (reproduced from Bourges (1998)). The background (lower line and open squares) was obtained from q scans across the magnetic line. The upper solid curve is a fit to $a + bF^2(\mathbf{Q})\sin^2(\pi zq_l)$, where $F(\mathbf{Q})$ is the Cu magnetic form factor. The modulation is not complete as even excitations are sizable at $q_l = 3.5, 7$, but with a magnitude five times smaller (Bourges 1998).

backgrounds) are only expected to obey the standard temperature dependence $1/[1 - \exp(-E/k_B T)]$ (see detailed discussion by Bourges *et al.* 1996). In the energy range of interest ($E > 40\text{ meV}$), this temperature dependence factor is close to unity and nearly independent of temperature for $T < 150\text{ K}$. Indeed, the normal-state neutron intensities of both YBCO (Bourges *et al.* 1996) and BSCCO (Fong *et al.* 1999, He *et al.* 2001) show a negligible temperature dependence for $T_c < T < 150\text{ K}$. For $E = E_r = 46\text{ meV}$ in Tl-2201, the factor $1/[1 - \exp(-E/k_B T)]$ decreases by 0.4% when the temperature is lowered from 99 to 27 K. If we take the non-magnetic background of 2500 counts per 2 h (He *et al.* 2002), the non-magnetic background decreases by 10 counts per 2 h when the temperature goes from 99 to 27 K, and by 60 counts per 2 h when the temperature goes from 150 to 99 K. The variation of the

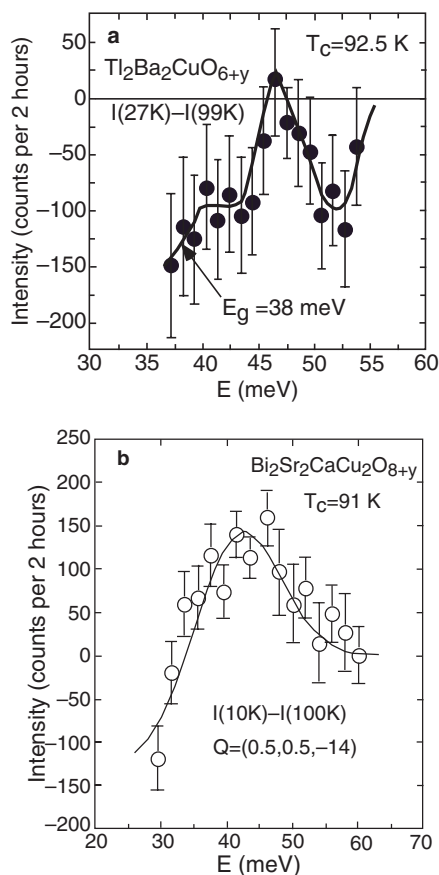


Figure 2. (a) The difference spectrum of the neutron intensities of single-layer TI-2201 crystals (with a total volume of 0.11 cm^3) at $T = 27 \text{ K}$ ($< T_c$) and $T = 99 \text{ K}$ ($> T_c$), and at wavevector $\mathbf{Q} = (0.5, 0.5, 12.25)$ (reproduced from He *et al.* (2002)). The solid line is a guide to the eye. The difference spectrum tends to zero at about 56 meV (about 10 meV higher than the resonance energy). This suggests that the non-magnetic background at 56 meV has negligible temperature dependence below 100 K . (b) The difference spectrum of the neutron intensities of optimally doped BSCCO crystals (with a total volume of 0.06 cm^3) at $T = 10 \text{ K}$ ($< T_c$) and $T = 100 \text{ K}$ ($> T_c$), and at wavevector $\mathbf{Q} = (0.5, 0.5, -14)$ (reproduced from Fong *et al.* (1999)). The difference spectrum goes to zero at 60 meV (about 16 meV higher than the resonance energy). This suggests that the non-magnetic background at 60 meV has negligible temperature dependence below 100 K .

non-magnetic background at $E = 46 \text{ meV}$ below 100 K is negligibly small compared with the magnetic resonance intensity (~ 150 counts per 2 h). Therefore, feature (e) identified for single-layer TI-2201 is well justified.

In order to further justify feature (e), we compare the ratios of the magnetic to the non-magnetic background signals in those neutron experiments on different compounds. From the neutron data, we find that the signal-to-background ratio is about 6% for TI-2201 (He *et al.* 2002), about 12% for an optimally doped BSCCO (Fong *et al.* 1999), about 6% for an overdoped BSCCO (He *et al.* 2001), and about 100% for an overdoped YBCO (Bourges *et al.* 1996). The signal-to-background ratio in the overdoped BSCCO is similar to that for TI-2201. But the

overdoped BSCCO shows a difference spectrum similar to that for the overdoped YBCO, where the signal-to-background ratio is larger than that for the overdoped BSCCO by a factor of 20. This suggests that, if feature (e) identified for TI-2201 were an artefact caused by a small signal-to-background ratio, one would not have observed the intrinsic difference spectra for the overdoped BSCCO. The fact that the difference spectra for the overdoped BSCCO are similar to that for YBCO suggests that one indeed finds the intrinsic magnetic difference spectra for the overdoped BSCCO even though the signal-to-background ratio is only 6%. There is no reason to believe that only the difference spectrum for TI-2201 is an artefact. Therefore, the pronounced difference between the difference spectrum of the single-layer TI-2201 and that of the double-layer BSCCO (compare figures 2(a) and (b)) is due to the fact that $I_{\text{odd}}^{\text{S}}(E_{\text{r}})/I_{\text{odd}}^{\text{N}}(E_{\text{r}}) \gg 1$ for the double-layer BSCCO, while $I^{\text{S}}(E_{\text{r}})/I^{\text{N}}(E_{\text{r}}) \sim 1$ for the single-layer TI-2201. Moreover, we will show below that, for the intraband scattering (even channel) in $\text{YBa}_2\text{Cu}_3\text{O}_{6.92}$, $I_{\text{even}}^{\text{S}}(E_{\text{r}})/I_{\text{even}}^{\text{N}}(E_{\text{r}}) = 0.72$, in good agreement with feature (e) for the single-layer TI-2201. This consistency gives further support to the thesis that feature (e) is intrinsic.

One may also argue that the glue that glues about 300 small crystals of TI-2201 on Al plates would cause a substantial decrease of the non-magnetic background below 100 K. If this argument were relevant, one would have observed a similar effect in overdoped $\text{Y}_{0.9}\text{Ca}_{0.1}\text{Ba}_2\text{Cu}_3\text{O}_{7-y}$ (YBCO-Ca) because 60 larger crystals of YBCO-Ca are also glued on Al plates (Pailhes *et al.* 2003). Because the total volume of YBCO-Ca crystals is larger than that of TI-2201 crystals by a factor of 3.2, one can readily show that the amount of glue for YBCO-Ca crystals is comparable to or even larger than that for TI-2201. This suggests that the effect of glue on the non-magnetic background in TI-2201 is similar to that in YBCO-Ca. From the data for YBCO-Ca (figures 2(a) and 3(a) of Pailhes *et al.* (2003)), one can clearly see that the difference spectrum at 50 meV is very close to zero. Because the magnetic signal at an energy that is about 10 meV higher than the resonance energy is independent of temperature below 100 K (see figure 1(a)), the nearly zero value of the difference spectrum at 50 meV implies that the non-magnetic background at 50 meV has negligible temperature dependence below 100 K in the case of YBCO-Ca. Even in the case of TI-2201 (see figure 2(a)), the difference spectrum tends to zero at about 56 meV (about 10 meV higher than the resonance energy), although one needs more data points in the vicinity of 56 meV to definitively address this issue. This indicates that the non-magnetic background at 56 meV has negligible temperature dependence below 100 K in the case of TI-2201.

We should mention that the normal-state magnetic intensities in figure 4 of He *et al.* (2002) are significantly underestimated. This is because the authors assume that the q width of the magnetic peak in the normal state is the same as that in the superconducting state (He *et al.* 2002). This assumption is unphysical. From figures 19(d) and (h) of Dai *et al.* (2001), one can clearly see that the q width of the magnetic peak in the normal state is a factor of 1.6 larger than that in the superconducting state in the case of underdoped $\text{YBa}_2\text{Cu}_3\text{O}_{6.8}$. Further, the q width increases with the increase of doping. With a much broader magnetic peak in the normal state, the q range (0.35–0.65 rlu) for the normal-state q -scan spectrum (see figure 2(b) of He *et al.* (2002)) is too narrow to obtain meaningful estimates of the non-magnetic background and the normal-state magnetic intensity. Moreover, the normal-state q -scan spectrum of $\text{YBa}_2\text{Cu}_3\text{O}_{6.8}$ is nearly featureless for the same

narrow q range (0.35–0.65 rlu), similar to the data of figure 2(b) of He *et al.* (2002). If one would fit the normal-state q -scan data only in this narrow q range (0.35–0.65 rlu) for $\text{YBa}_2\text{Cu}_3\text{O}_{6.8}$ and assume the same q width as that in the superconducting state, one would find that the normal-state magnetic intensity is underestimated by a factor of 4. Such a significant underestimate may also be true for the normal-state magnetic intensities of Tl-2201. He *et al.* (2002) should have extended their measurements to a wider q range to obtain reliable estimates of the non-magnetic background and the normal-state magnetic intensities.

Since the magnetic signals in both normal and superconducting states strongly depend on doping, as clearly seen in YBCO (Bourges 1998), comparison of the resonance peak intensities and spectral weights among different compounds should be made carefully. For Tl-2201, there is some indication of a broad peak centred around \mathbf{Q}_{AF} even above T_c (He *et al.* 2002), as observed in underdoped YBCO (Bourges 1998, Dai *et al.* 2001). This suggests that Tl-2201 is slightly underdoped so that the magnetic intensity in the normal state should be close to that for slightly underdoped $\text{YBa}_2\text{Cu}_3\text{O}_{6.92}$. This is because both compounds have a similar ratio T_c/T_{cm} and thus a similar doping level (where T_{cm} is the superconducting transition at optimal doping). As seen from figure 1(a), the normal-state magnetic intensity at 40 meV is about $100 \mu_B^2/\text{eV}$ per Cu in slightly underdoped $\text{YBa}_2\text{Cu}_3\text{O}_{6.92}$. The resonance peak intensity for Tl-2201 can be estimated to be about $120 \mu_B^2/\text{eV}$ per Cu from the resonance spectral weight of $0.7 \mu_B^2$ per Cu (He *et al.* 2002). Therefore, the resonance peak intensity for Tl-2201 is close to the normal-state magnetic intensity for the slightly underdoped $\text{YBa}_2\text{Cu}_3\text{O}_{6.92}$. Since the normal-state magnetic intensity for Tl-2201 should be similar to that for the slightly underdoped $\text{YBa}_2\text{Cu}_3\text{O}_{6.92}$, then $I^{\text{S}}(E_r)/I^{\text{N}}(E_r) \simeq 1.2$ for this single-layer Tl-2201. This is in good agreement with feature (e) deduced independently from the difference spectrum (figure 2(a)). Moreover, we find that the resonance peak intensity for Tl-2201 ($\sim 120 \mu_B^2/\text{eV}$ per Cu) is a factor of about 3 smaller than the resonance peak intensity for the slightly underdoped $\text{YBa}_2\text{Cu}_3\text{O}_{6.92}$ ($\sim 330 \mu_B^2/\text{eV}$ per Cu). Similarly, the resonance spectral weight for Tl-2201 is also a factor of 3 smaller than that for the slightly underdoped $\text{YBa}_2\text{Cu}_3\text{O}_{6.92}$.

The important features identified above should place strong constraints on theories for high-temperature superconductivity in cuprates. Any correct theories should be able to explain all the magnetic resonance features in a consistent and quantitative way. In a more exotic approach (Delmer and Zhang 1995), the neutron data are interpreted in terms of a collective mode in the spin-triplet particle–particle channel, which couples to the particle–hole channel in the superconducting state with d-wave OP. This model predicts that the resonance peak energy E_r is proportional to the doping level p , in disagreement with feature (d): E_r does not increase with increasing p in the overdoped range, but is proportional to T_c as $E_r/k_B T_c \simeq 5.2$ (He *et al.* 2001). Moreover, this model predicts (Tchernyshyov *et al.* 2001) that $E_r > 2\Delta_{\text{M}}$ (where Δ_{M} is the maximum d-wave gap), which contradicts experiment. Other theories based on spin–fermion interactions also show that E_r increases monotonically with increasing p (Morr and Pines 1998, Abanov and Chubukov 1999), in disagreement with feature (d).

Alternatively, feature (d) is consistent with a simple particle–hole excitation across the superconducting gap within an itinerant magnetism model. This is because the particle–hole excitation energy increases with the superconducting gap which, in turn, should be proportional to T_c , at least in the overdoped range. This itinerant

magnetism model is also supported by very recent Fourier transform-scanning tunnelling spectroscopic (FT-STs) studies on a nearly optimally doped BSCCO (McElroy *et al.* 2003), which show that the quasiparticles in the superconducting state exhibit particle–hole mixing similar to that of conventional Fermi-liquid superconductors. These FT-STs results thus provide evidence for Fermi-liquid behaviour in the superconducting state of optimally doped and overdoped cuprates. Here we quantitatively explain all these neutron data (Bourges *et al.* 1995, 1996, 1999, Fong *et al.* 1995, 1999, Bourges 1998, Dai *et al.* 2001, He *et al.* 2001, 2002) in terms of an order parameter (OP) that has an extended s-wave symmetry (Zhao 2001, Brandow 2002) and opposite sign in the bonding and antibonding electron bands formed within the Cu_2O_4 bilayers (Mazin and Yakovenko 1995). In our model, the neutron resonance peak is due to excitations of electrons from the extended saddle points below the Fermi level to the superconducting gap edge above the Fermi level.

Within the itinerant magnetism model, the neutron scattering intensity at wave-vector \mathbf{q} and energy E is proportional to the imaginary part of the dynamic electron spin susceptibility, $\chi''(\mathbf{q}, E)$. Qualitatively, neglecting the Bardeen–Cooper–Schrieffer (BCS) coherence factor, the bare imaginary part of the spin susceptibility, $\chi''_0(\mathbf{q}, E)$, is proportional to the joint density of states $A(\mathbf{q}, E) = \sum_{\mathbf{k}} \delta(E - E_{\mathbf{k}+\mathbf{q}} - E_{\mathbf{k}})$, where $E_{\mathbf{k}} = (\epsilon_{\mathbf{k}}^2 + \Delta_{\mathbf{k}}^2)^{1/2}$ is the quasiparticle dispersion law below T_c , $\epsilon_{\mathbf{k}}$ is the electronic band dispersion, and $\Delta_{\mathbf{k}}$ is the order parameter (Mazin and Yakovenko 1995). The two-particle energy $E_2(\mathbf{k}, \mathbf{q}) = E_{\mathbf{k}+\mathbf{q}} + E_{\mathbf{k}}$ has a minimum and several saddle points for a fixed \mathbf{q} . The minimum defines the threshold energy, or spin gap energy E_g , which is achieved at vector \mathbf{k} and $\mathbf{k} + \mathbf{q}$ such that both \mathbf{k} and $\mathbf{k} + \mathbf{q}$ belong to the Fermi surface and thus $E_g = 2\Delta_{\mathbf{k}}$ (Mazin and Yakovenko 1995).

The joint density of states has divergences at the extended saddle points (Mazin and Yakovenko 1995). The divergent peak in $\chi''_0(\mathbf{q}, \omega)$ occurs because of transitions between the occupied states located in the extended saddle points below E_F and empty quasiparticle states at the superconducting gap edge above E_F . The saddle points produce Van Hove singularities in the quasiparticle density of states in the superconducting state at an energy of $[(\epsilon_{\mathbf{k}}^{\text{VH}})^2 + \Delta_{\mathbf{k}}^2]^{1/2}$ and the superconducting condensate creates a sharp coherence peak in the quasiparticle density of states at the gap edge. Thus, the divergence in the joint density of states in the superconducting state is then located at energy $E^* = \Delta_{\mathbf{k}+\mathbf{q}} + [(\epsilon_{\mathbf{k}}^{\text{VH}})^2 + \Delta_{\mathbf{k}}^2]^{1/2}$. This simple expression for E^* has been verified by numerical calculations in the case of an isotropic s-wave order parameter (Mazin and Yakovenko 1995).

In figure 3 we plot the Fermi surface for a slightly underdoped BSCCO, which is inferred by extending a portion of the Fermi surface determined by angle-resolved photoemission spectroscopy (ARPES) (White *et al.* 1996). There are extended saddle points that are located near $(\pm\pi, 0)$ and $(0, \pm\pi)$, as shown by ARPES (Dessau *et al.* 1993). A solid line in figure 3 represents a segment of the extended saddle points very close to the Fermi surface. Other portions of the saddle points (e.g. along the line from $(0, 0)$ to $(\pi, 0)$) are significantly away from the Fermi surface (Dessau *et al.* 1993) and not shown in the figure. If we only consider the magnetic excitations at a fixed wavevector that corresponds to the antiferromagnetic wavevector \mathbf{Q}_{AF} , only four electron wavevectors at the Fermi surface are connected by \mathbf{Q}_{AF} , as indicated by arrow 1 in figure 3. Each of these vectors forms an angle of θ_r with respect to the Cu–O bonding direction. The electron transitions from the occupied states located at the extended saddle points below E_F to empty quasiparticle states at the superconducting gap edge above E_F are indicated by arrow 2. Because the quasiparticle

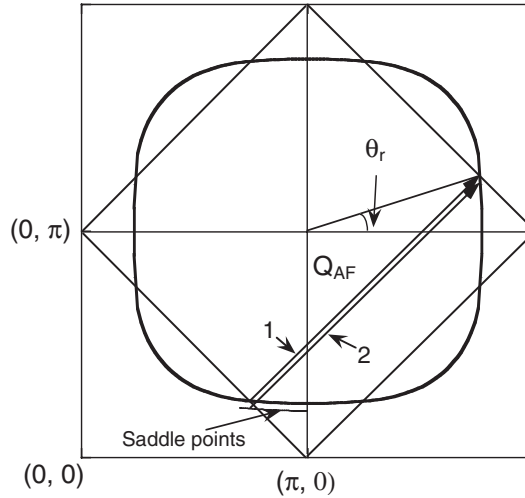


Figure 3. The Fermi surface for a slightly underdoped BSCCO with $T_c = 88$ K. This Fermi surface is extrapolated from a part of the Fermi surface determined by ARPES (White *et al.* 1996) using symmetry arguments. Arrow 1 indicates electron transitions from the occupied states in the superconducting gap edge below E_F to empty quasiparticle states at the gap edge above E_F . Arrow 2 indicates electron transitions from the occupied states located in the extended saddle points below E_F to empty quasiparticle states in the superconducting gap edge above E_F .

densities of states at the gap edge and the saddle points are divergent at zero temperature, such transitions will produce a sharp resonance peak at $E_r = \Delta_{\mathbf{k}+\mathbf{Q}_{AF}} + [(\epsilon_{\mathbf{k}}^{\text{VH}})^2 + \Delta_{\mathbf{k}}^2]^{1/2}$ (Mazin and Yakovenkov 1995).

Both $E_g(\mathbf{Q}_{AF})$ and $E_r(\mathbf{Q}_{AF})$ can be rewritten in terms of θ_r as

$$E_g(\mathbf{Q}_{AF}) = 2\Delta(\theta_r) \quad (1)$$

and

$$E_r(\mathbf{Q}_{AF}) = \Delta(\theta_r) + \sqrt{[\Delta(\theta_r)]^2 + (\epsilon_r^{\text{VH}})^2}. \quad (2)$$

Here, $\{[\Delta(\theta_r)]^2 + (\epsilon_r^{\text{VH}})^2\}^{1/2}$ is the energy of a saddle point below the Fermi level along the θ_r direction. One should note that equation (2) is valid only if the saddle points are very close to the Fermi surface, as is the case here.

We now consider the BCS coherence factor that has been ignored in the above discussions. The BCS coherence factor is given by (Schrieffer 1988)

$$\xi(\mathbf{q}, \mathbf{k}) = \frac{1}{2} \left(1 - \frac{\epsilon_{\mathbf{k}} \epsilon_{\mathbf{k}+\mathbf{q}} + \Delta_{\mathbf{k}+\mathbf{q}} \Delta_{\mathbf{k}}}{E_{\mathbf{k}} E_{\mathbf{k}+\mathbf{q}}} \right). \quad (3)$$

For $\epsilon_{\mathbf{k}} \ll \Delta_{\mathbf{k}}$ and $\epsilon_{\mathbf{k}+\mathbf{q}} \ll \Delta_{\mathbf{k}+\mathbf{q}}$, the BCS coherence factor is close to 1 when $\Delta_{\mathbf{k}+\mathbf{q}}$ and $\Delta_{\mathbf{k}}$ have opposite sign, but is close to zero when $\Delta_{\mathbf{k}+\mathbf{q}}$ and $\Delta_{\mathbf{k}}$ have the same sign. The coherence factor is not negligible for $\epsilon_{\mathbf{k}} \simeq \Delta_{\mathbf{k}}$ and $\epsilon_{\mathbf{k}+\mathbf{q}} = 0$ even if $\Delta_{\mathbf{k}+\mathbf{q}}$ and $\Delta_{\mathbf{k}}$ have the same sign.

For a single-layer compound with d-wave order parameter symmetry, $\Delta_{\mathbf{k}+\mathbf{Q}_{AF}}$ and $\Delta_{\mathbf{k}}$ have opposite sign so that the BCS coherence factor $\simeq 1$ and thus $I^S(E_r)/I^N(E_r) \gg 1$ (Brinckmann and Lee 1999). Therefore, the experimental observation of $I^S(E_r)/I^N(E_r) \sim 1.0$ in the single-layer Tl-2201 (He *et al.* 2002) rules out the d-wave

order parameter. Alternatively, for a single-layer compound with an s-wave symmetry, $\Delta_{\mathbf{k}+\mathbf{Q}_{AF}}$ and $\Delta_{\mathbf{k}}$ have the same sign, so the BCS coherence factor could be much less than 1. This may lead to $I^S(E_r)/I^N(E_r) \sim 1$, in agreement with feature (e). Hence, only the intralayer (inraband) s-wave symmetry is compatible with feature (e): $I^S(E_r)/I^N(E_r) \sim 1.0$. On the other hand, if extended saddle points are significantly below the Fermi level, the BCS coherence factor will be substantial even for intralayer (inraband) magnetic scattering in the case of s-wave gap symmetry. Then $I^S(E_r)/I^N(E_r)$ could be much larger than 1 in this special case. Therefore, the observation of $I^S(E_r)/I^N(E_r) \gg 1$ for the intralayer (inraband) magnetic scattering is consistent with either s-wave or d-wave gap symmetry.

For a double-layer compound, interactions within Cu_2O_4 bilayers yield bonding and antibonding bands. Transitions between electronic states of the same type (bonding-to-bonding or antibonding-to-antibonding) and those of opposite types are characterized by even or odd symmetry, respectively, under exchange of two adjacent CuO_2 layers. As a result, the magnetic excitations between different bands correspond to odd channel excitations, while the excitations within the same band correspond to even channel excitations (Bourges 1998). If the order parameters in the bonding and antibonding bands have the same sign, the magnetic resonance intensities in both channels should be similar for an intraband pairing symmetry of either s wave or d wave. This is because the BCS coherence factors for both channels are the same in this case. On the other hand, if the order parameter has an s-wave symmetry and opposite sign in the bonding and antibonding electron bands, the magnetic resonance intensity in the odd channel will be much larger than that in the even channel due to the large difference in their BCS coherence factors. Therefore, only if the order parameter has an s-wave symmetry and opposite sign in the bonding and antibonding electron bands can the observed feature (c) $I_{\text{odd}}^S(E_r)/I_{\text{even}}^S(E_r) = 5$ for the slightly underdoped YBCO and $I_{\text{odd}}^S(E_r)/I_{\text{even}}^S(E_r) > 10$ for the overdoped YBCO (Bourges *et al.* 1996) be explained within the itinerant magnetism approach.

Based on the t-J model and d-wave pairing symmetry, Brinckmann and Lee (2001) have recently attempted to account for feature (c) using a very unrealistic parameter: $J_{\perp}/J_{\parallel} = 0.6$ (where J_{\parallel} and J_{\perp} are the effective intralayer and interlayer antiferromagnetic exchange energies, respectively). For undoped YBCO, neutron experiments (Bourges 1998) shows that $J_{\perp}/J_{\parallel} = 0.1$, which is far less than 0.6 used in the calculation (Brinckmann and Lee 2001). Further, the value of J_{\perp}/J_{\parallel} will be negligible if J_{\parallel} remains substantial and the optical magnon gap ($\propto (J_{\parallel}J_{\perp})^{1/2}$) goes to zero, which should be the case for optimally doped and overdoped YBCO. Neutron data for underdoped YBCO (Fong *et al.* 2000) show that the optical magnon gap is about 50 meV for $\text{YBa}_2\text{Cu}_3\text{O}_{6.5}$ and is reduced to about 25 meV for $\text{YBa}_2\text{Cu}_3\text{O}_{6.7}$. If we linearly extrapolate the optical magnon gap with the oxygen content, the gap will tend to zero in $\text{YBa}_2\text{Cu}_3\text{O}_y$ for $y > 0.9$, implying that $J_{\perp}/J_{\parallel} \ll 0.1$ for optimally doped and overdoped cuprates.

Using a more realistic parameter for J_{\perp} and the d-wave pairing symmetry, Millis and Monien (1996) appear to be able to explain feature (c). They showed that the resonance spectral weights in the odd and even channels are related to the difference between the resonance energy E_r and the particle-hole spin excitation energy $2\Delta(\theta_r)$ at \mathbf{Q}_{AF} , i.e. $W^{\text{odd}}/W^{\text{even}} = [2\Delta(\theta_r) - E_r^{\text{odd}}]/[2\Delta(\theta_r) - E_r^{\text{even}}]$. Here, $2\Delta(\theta_r)$ must be larger than both E_r^{even} and E_r^{odd} (Millis and Monien 1996). The INS data of $\text{Y}_{0.9}\text{Ca}_{0.1}\text{Ba}_2\text{Cu}_3\text{O}_{7-y}$ would be consistent with this theoretical model if one would

choose an unrealistic parameter $2\Delta(\theta_r) = 49$ meV (Pailhes *et al.* 2003). As discussed below, θ_r is about 15° for slightly overdoped cuprates, so that $2\Delta(\theta_r) = 1.73\Delta_M$ (where Δ_M is the maximum d-wave gap). The intrinsic tunneling spectra, which are not susceptible to surface deterioration, can provide the most reliable determination of the bulk superconducting gap (Krasnov *et al.* 2000). From the intrinsic tunneling spectra, one finds that $2\Delta_M/k_B T_c = 8.09$ for the optimally doped BSCCO with $T_c = 94$ K (Krasnov *et al.* 2000), $2\Delta_M/k_B T_c = 6.73$ for a slightly overdoped BSCCO with $T_c = 89$ K (Krasnov *et al.* 2000), and $2\Delta_M/k_B T_c = 5.37$ for an overdoped BSCCO with $T_c = 80$ K (Yurgens *et al.* 1999). It is apparent that $2\Delta_M/k_B T_c$ decreases almost linearly with T_c in the overdoped range. Using the fitted curve of $2\Delta_M/k_B T_c$ versus T_c , we estimate $2\Delta_M/k_B T_c = 6.04$ and $2\Delta(\theta_r) = 38.6$ meV for $Y_{0.9}Ca_{0.1}Ba_2Cu_3O_{7-y}$ with $T_c = 85.5$ K. Similarly, we can obtain $2\Delta_M/k_B T_c = 5.66$ and $2\Delta(\theta_r) = 35.1$ meV for overdoped BSCCO with $T_c = 83$ K. An INS experiment on $Y_{0.9}Ca_{0.1}Ba_2Cu_3O_{7-y}$ (Pailhes *et al.* 2003) indicates $E_r^{\text{even}} = 43$ meV $> 2\Delta(\theta_r)$, which contradicts the theoretical model (Millis and Monien 1996). For overdoped BSCCO with $T_c = 83$ K, $E_r^{\text{odd}} = 38$ meV (He *et al.* 2001) and thus $E_r^{\text{even}} = 45$ meV by analogy with the case of $Y_{0.9}Ca_{0.1}Ba_2Cu_3O_{7-y}$. Both E_r^{even} and E_r^{odd} in this overdoped BSCCO are far larger than $2\Delta(\theta_r)$, in contradiction with the d wave model (Millis and Monien 1996). Moreover, the predicted spectral weight from this d-wave model is $W^{\text{odd}} = 16\pi[2\Delta(\theta_r) - E_r^{\text{odd}}]/J_{\text{parallel}}A$ (μ_B^2/Cu) (Millis and Monien 1996). Using the parameters: $2\Delta(\theta_r) = 49$ meV (Pailhes *et al.* 2003), $E_r^{\text{odd}} = 36$ meV (Pailhes *et al.* 2003), $J_{\text{parallel}} = 100$ meV, and $A = 0.1$ (Millis and Monien 1996), we find $W^{\text{odd}} = 65.3\mu_B^2/\text{Cu}$, which is larger than the measured value of $0.40\mu_B^2/\text{Cu}$ (Pailhes *et al.* 2003) by a factor of 163.

For the underdoped $YBa_2Cu_3O_{6.7}$, the even-channel magnetic intensity in the normal state is a factor of 2.0–2.5 lower than the odd-channel intensity for $E = 40$ meV, which is about 15 meV above the optical magnon gap (Fong *et al.* 2000). This implies that the interlayer antiferromagnetic correlation does not influence magnetic excitations well above the optical magnon gap (Fong *et al.* 2000). Since the optical magnon gaps for optimally doped and overdoped YBCO are much smaller than that for underdoped $YBa_2Cu_3O_{6.7}$, one should expect that $I_{\text{odd}}^N(E)/I_{\text{even}}^N(E) \simeq 1$ for $E \simeq 40$ meV in optimally doped and overdoped YBCO. Thus, the observed feature (c): $I_{\text{odd}}^S(E_r)/I_{\text{even}}^S(E_r) \gg 1$ for optimally doped and overdoped YBCO can only be explained by an OP that has s-wave symmetry and opposite sign in the bonding and antibonding electron bands.

For the slightly underdoped $YBa_2Cu_3O_{6.92}$, we can also deduce the value of $I_{\text{even}}^S(E_r)/I_{\text{even}}^N(E_r)$ using the measured $I_{\text{odd}}^S(E_r)/I_{\text{odd}}^N(E_r) = 3.6$ and $I_{\text{odd}}^S(E_r)/I_{\text{even}}^S(E_r) = 5$, and the inferred $I_{\text{odd}}^N(E_r)/I_{\text{even}}^N(E_r) \simeq 1$ (see above discussion). From the measured $I_{\text{odd}}^S(E_r)/I_{\text{even}}^S(E_r) = 5$, we have $I_{\text{even}}^S(E_r) = 0.2I_{\text{odd}}^S(E_r)$ and thus $I_{\text{even}}^S(E_r)/I_{\text{even}}^N(E_r) \simeq 0.2I_{\text{odd}}^S(E_r)/I_{\text{odd}}^N(E_r) = 0.72$. This value is close to that deduced for the single-layer Tl-2201 ($\simeq 1$). These results consistently suggest that the intraband neutron intensity at E_r in the superconducting state is close to that in the normal state. This unique and important feature identified here rules out d-wave order parameter symmetry because d-wave symmetry predicts (Brinckmann and Lee 1999, 2001) that $I_{\text{even}}^S(E_r)/I_{\text{even}}^N(E_r) \gg 1$ for bilayer compounds and $I^S(E_r)/I^N(E_r) \gg 1$ for single-layer compounds.

From equations (1) and (2), it is easy to calculate E_g and E_r if one knows the gap function $\Delta(\theta)$ and the θ_r value. From the measured Fermi surface, one can readily determine θ_r . For example, we find $\theta_r = 18.4^\circ$ for a slightly underdoped BSCCO

from figure 3. For optimally doped cuprates, we get $\theta_r \simeq 16.0^\circ$. If we would use an isotropic s-wave gap function $\Delta(\theta) = 28$ meV for a slightly overdoped YBCO, we would have $E_g = 56$ meV and $E_r > 56$ meV, which are far larger than the measured $E_g = 33$ meV and $E_r = 40$ meV (Bourges *et al.* 1996). If we would use a d-wave gap function $\Delta(\theta) = 28 \cos 2\theta$ meV, we would have $E_g = 47.5$ meV and $E_r > 47.5$ meV, which are also far larger than the measured values. Thus, one cannot quantitatively explain the neutron data in terms of d-wave and isotropic s-wave symmetries.

Alternatively, an extended s wave with eight line nodes (A_{1g} symmetry) is in quantitative agreement with two-thirds of the experiments that were designed to test the order-parameter symmetry for hole-doped cuprates (Zhao 2001). The remaining one-third (e.g., tricrystal grain-boundary Josephson junction experiments) are explained qualitatively by Zhao (2001) and Brandow (2002). In table 1, we compare nearly all the experiments used to test the OP symmetry with the extended s-wave, d-wave, and isotropic s-wave models. In both extended s-wave and isotropic s-wave models, the order parameters are assumed to have opposite sign in the bonding and antibonding electron bands formed within the Cu_2O_4 bilayers (Mazin and Yakovenkov 1995). Detailed comparisons with other experiments are made by Zhao (2001). From table 1, one can see that the neutron data alone provide a definitive answer to the intrinsic, bulk OP symmetry because INS is a bulk-

Table 1. Comparison of experiments with extended s wave, d wave, and isotropic s wave. In both extended and isotropic s-wave models, the order parameters are assumed to have opposite sign in the bonding and antibonding electron bands formed within the Cu_2O_4 bilayers. DA, definitive agreement; A, agreement; QA, qualitative agreement; PA, possible agreement; D, disagreement; DD, definitive disagreement.

INS data	Extended s wave	d wave	Isotropic s wave
Feature (a): $I^S(E_r)/I^N(E_r) = 3.6$ for YBCO	DA	DA	DA
Feature (c): $I^S_{\text{odd}}(E_r)/I^S_{\text{even}}(E_r) = 5$ for YBCO	DA	DD	DA
Feature (e): $I^S(E_r)I^N(E_r) < 1$ for Tl-2201	DA	DD	DA
The magnitudes of E_r and E_g	DA	DD	DD
Spin gap in $\text{La}_{2-x}\text{Sr}_x\text{CuO}_4$	DA	DD	DD
Other data			
Penetration depth	DA	QA	DD
Thermal conductivity	DA	QA	DD
Specific heat	DA	QA	DD
Nonlinear Meissner effect	DA	QA	DD
ARPES (underdoped)	A	A	DD
ARPES (overdoped)	DA	DD	DD
Quasiparticle tunneling (underdoped)	PA	PA	DD
Quasiparticle tunneling (overdoped)	DA	DD	DD
Raman scattering (underdoped)	PA	PA	DD
Raman scattering (overdoped)	DA	DD	PA
NMR/NQR	A	A	DD
Andreev reflection	A	PA	DD
Pb/c-axis YBCO Josephson junction	A	D	A
c-axis BSCCO twist Josephson junction	DA	DD	PA
Corner SQUID/Josephson junction	PA	PA	PA
Tricrystal/tetracrystal Josephson junctions	PA	PA	PA

phase- and angle-sensitive technique. Other bulk- and non-phase-sensitive experiments provide complementary support to the present conclusions. The phase- and surface-sensitive experiments cannot definitively determine the intrinsic bulk OP symmetry because the surface OP might be different from the bulk OP (Zhao 2001).

For a slightly overdoped YBCO, more than six independent experiments consistently suggest that (Zhao 2001) the gap function is $\Delta(\theta) = 24.5(\cos 4\theta + 0.225)$ meV. Substituting $\theta_r = 16^\circ$ into the gap function, we get $\Delta(\theta_r) = 16.3$ meV, and thus $E_g = 32.6$ meV, in quantitative agreement with the measured value (32–33 meV).

In our model, the position of the extended saddle point along the θ_r direction is located at $E_r - E_g/2$ in the superconducting state (see equations (1) and (2)). For optimally doped YBCO with $E_r = 41$ meV and $E_g = 32$ meV, we find that the saddle point in the superconducting state is located at an energy of 25 meV below the Fermi level. This is in agreement with the ARPES studies (King *et al.* 1994), which suggest that the Fermi level in the superconducting state for optimally doped cuprates is ≤ 30 meV above the extended saddle points that have the same energy over a large momentum space (Dessau *et al.* 1993). Further, electronic Raman scattering spectra in $\text{YBa}_2\text{Cu}_4\text{O}_8$ have been used to determine the energy of the extended saddle points more accurately (Sherman and Misochko 1999). At 10 K (well below T_c), the energy of the extended saddle points is found to be 24.3 meV below the Fermi level, in excellent agreement with the result predicted by our model from the INS data ($\simeq 25$ meV).

We have identified a unique and important feature, $I^S(E_r)/I^N(E_r) \simeq 1.0$, for intralayer and intraband magnetic scattering. This feature unambiguously rules out d-wave OP symmetry. The unambiguous determination of the intrinsic extended s-wave pairing symmetry for hole-doped cuprates places strong constraints on the pairing mechanism for high-temperature superconductivity. A recent calculation suggests that high-energy Cu–O charge fluctuations can lead to an attractive interaction between conduction electrons and the pairing symmetry may be of extended s wave (A_{1g}) (Gulacsi and Chan 2001).

Indeed, precise thermal-difference reflectance spectra of several cuprate superconductors ($T_c = 105$ – 120 K) exhibit pronounced features at photon energies of about 2.0 eV, which may be related to the Cu–O charge fluctuations (Holcomb *et al.* 1994, 1996). These features can be well described within Eliashberg theory with an electron–boson coupling constant λ_{ch} of about 0.40. In order to explain a superconducting transition temperature of 105–120 K, the authors simulated (Holcomb *et al.* 1996) an electron–phonon coupling feature at 50 meV with a coupling constant λ_{ph} of about 1.0. This Eliashberg model’s simulated electron–phonon coupling agrees well with the results obtained from first-principle calculations (Pickett 1989).

The contribution of this 2 eV component may be equivalent to a *negative* Coulomb pseudopotential μ^* within Eliashberg theory (Zhao *et al.* 2001). Using a realistic electron–phonon coupling spectral weight deduced from tunneling spectra and $\mu^* = -0.15$, and taking into account a polaronic effect, Zhao *et al.* (2001) were able to explain the negligible isotope effect on T_c and the magnitudes of T_c and the superconducting gap for optimally doped 90 K superconductors.

In summary, we have identified several important features in the neutron scattering data of cuprates that are difficult to explain in terms of d-wave and isotropic s-wave order parameters. Alternatively, we show that the neutron data are in quantitative agreement with an order parameter that has an extended s-wave (A_{1g})

symmetry and opposite sign in the bonding and antibonding electron bands formed within the Cu_2O_4 bilayers. This A_{1g} pairing symmetry may be compatible with a charge-fluctuation-mediated pairing mechanism. The high-temperature superconductivity in cuprates may be due to the combination of strong electron-phonon coupling and substantial electron-charge-fluctuation coupling (Holcomb *et al.* 1994, 1996, Zhao *et al.* 2001).

REFERENCES

- ABANOV, A., and CHUBUKOV, A. V., 1999, *Phys. Rev. Lett.*, **83**, 1652.
- BOURGES, P., 1998, *The Gap Symmetry and Fluctuations in High Temperature Superconductors*, NATO ASI Series, Physics, vol. 371, edited by J. Bok, G. Deutscher, D. Pavuna and S. A. Wolf (New York: Plenum Press), p. 349.
- BOURGES, P., REGNAULT, L. P., SIDIS, Y., and VETTER, C., 1996, *Phys. Rev. B*, **53**, 876.
- BOURGES, P., SIDIS, Y., FONG, H. F., KEIMER, B., REGNAULT, L. P., BOSSY, J., IVANOV, A. S., MILIUS, D. L., and AKSAY, I. A., 1999, *High Temperature Superconductivity*, edited by S. E. Barnes; J. Ashkenazi, J. L. Cohn, and F. Zuo (Amsterdam: American Institute of Physics), p. 207.
- BOURGES, P., SIDIS, Y., HENNION, B., VILLENEUVE, R., COLLIN, G., and MARUCCO, J. F., 1995, *Physica B*, **213-214**, 48.
- BRANDOW, B. H., 2002, *Phys. Rev. B*, **65**, 054503.
- BRINCKMANN, J., and LEE, P. A., 1999, *Phys. Rev. Lett.*, **82**, 2915; 2001, *Phys. Rev. B*, **65**, 014502.
- CHIAO, M., HILL, R. W., LUPIEN, C., TAILLEFER, L., LAMBERT, P., GAGNON, R., and FOURNIER, P., 2000, *Phys. Rev. B*, **62**, 3554.
- DAI, P. C., MOOK, H. A., HUNT, R. D., and DOGAN, F., 2001, *Phys. Rev. B*, **63**, 054525.
- DEMLER, E., and ZHANG, S. C., 1995, *Phys. Rev. Lett.*, **75**, 4126.
- DESSAU, D. S., SHEN, Z.-X., KING, D. M., MARSHALL, D. S., LOMBARDO, L. W., DICKINSON, P. H., LOESER, A. G., DICARLO, J., PARK, C.-H., KAPITULNIK, A., and SPICER, W. E., 1993, *Phys. Rev. Lett.*, **71**, 2781.
- FONG, H. F., BOURGES, P., SIDIS, Y., REGNAULT, L. P., BOSSY, J., IVANOV, A., MILIUS, D. L., AKSAY, I. A., and KEIMER, B., 2000, *Phys. Rev. B*, **61**, 14773.
- FONG, H. F., BOURGES, P., SIDIS, Y., REGNAULT, L. P., IVANOV, A., GUK, G. D., KOSHIZUKA, N., and KEIMER, B., 1999, *Nature (London)*, **398**, 588.
- FONG, H. F., KEIMER, B., ANDERSON, P. W., REZNIK, D., DOGAN, F., and AKSAY, I. A., 1995, *Phys. Rev. Lett.*, **75**, 316.
- GULACSI, M., and CHAN, R. J., 2001, *J. Supercond.*, **14**, 651, and private communication with M. Gulacsi.
- HARDY, W. N., BONN, D. A., MORGAN, D. C., LIANG, R.-X., and ZHANG, K., 1993, *Phys. Rev. Lett.*, **70**, 3999.
- HE, H., BOURGES, P., SIDIS, Y., ULRICH, C., REGNAULT, L. P., PAILHES, S., BERZIGIAROVA, N. S., KOLESNIKOV, N. N., and KEIMER, B., 2002, *Science*, **295**, 1045.
- HE, H., SIDIS, Y., BOURGES, P., GU, G. D., IVANOV, A., KOSHIZUKA, N., LIANG, B., LIN, C. T., REGNAULT, L. P., SCHOENHERR, E., and KEIMER, B., 2001, *Phys. Rev. Lett.*, **86**, 1610.
- HOLCOMB, M. J., COLLMAN, J. P., and LITTLE, W. A., 1994, *Phys. Rev. Lett.*, **73**, 2360.
- HOLCOMB, M. J., PERRY, C. L., COLLMAN, J. P., and LITTLE, W. A., 1996, *Phys. Rev. B*, **53**, 6734.
- KING, D. M., SHEN, Z.-X., DESSAU, D. S., MARSHALL, D. S., PARK, C. H., SPICER, W. E., PENG, J. L., LI, Z. Y., and GREENE, R. L., 1994, *Phys. Rev. Lett.*, **73**, 3298.
- KRASNOV, V. M., YURGENS, A., WINKLER, D., DELSING, P., and CLAESON, T., 2000, *Phys. Rev. Lett.*, **84**, 5860.
- MAZIN, I. I., and YAKOVENKO, V. M., 1995, *Phys. Rev. Lett.*, **75**, 4134.
- MC ELROY, K., SIMMONDS, R. W., HOFFMAN, J. E., LEE, D.-H., ORENSTEIN, J., EISAKI, H., UCHIDA, S., and DAVIS, J. C., 2003, *Nature (London)*, **422**, 592.
- MILLIS, A. J., and MONIEN, H., 1996, *Phys. Rev. B*, **54**, 16172.
- MORR, D. K., and PINES, D., 1998, *Phys. Rev. Lett.*, **81**, 1086.
- PAILHES, S., SIDIS, Y., BOURGES, P., ULRICH, C., HINKOV, V., REGNAULT, L. P., IVANOV, A., LIANG, B., LIN, C. T., BERNHARD, C., and KEIMER, B., 2003, cond-mat/0308394.

- PICKETT, W. E., 1989, *Rev. mod. Phys.*, **61**, 434.
- SCHRIEFFER, J. R., 1988, *Theory of Superconductivity*, Frontiers in Physics, vol. 20 (New York: Addison Wesley).
- SHERMAN, E. YA., and MISOCHKO, O. V., 1999, *Phys. Rev. B*, **59**, 195.
- TCHERNYSHYOV, O., NORMAN, M. R., and CHUBUKOV, A. V., 2001, *Phys. Rev. B*, **63**, 144507.
- WHITE, P. J., SHEN, Z.-X., KIM, C., HARRIS, J. M., LOESER, A. G., FOURNIER, P., and KAPITULNIK, A., 1996, *Phys. Rev. B*, **54**, R15669.
- YURGENS, A., WINKLER, D., CLAESON, T., HWANG, S. J., and CHOY, J. H., 1999, *Int. J. mod. Phys. B*, **13**, 3758.
- ZHAO, G. M., 2001, *Phys. Rev. B*, **64**, 024503.
- ZHAO, G. M., KIRTIKAR, V., and MORRIS, D. E., 2001, *Phys. Rev. B*, **63**, R220506.